Eur Biophys J (2011) 40:1225–1235
DOI 10.1007/s00249-011-0717-0

ORIGINAL PAPER

How soft are biological helices? A measure of axial and lateral force constants in folate quadruplexes by high-pressure X-ray diffraction

**Francesco Federiconi · Michele Mattioni ·
Enrico J. Baldassarri · Maria Grazia Ortore ·
Paolo Mariani**

Received: 7 March 2011 / Revised: 14 May 2011 / Accepted: 20 May 2011 / Published online: 29 June 2011

Abstract Alkaline folates self-associate in aqueous solutions to form columnar lyotropic phases. Such phases are made by quadruplexes, which are supramolecular helicoidal structures formed by a stacked array of folate tetramers. High-pressure synchrotron X-ray diffraction is used to analyze alkaline folate quadruplex stability and energetics. Diffraction data show that both inter-helical lateral and tetramer stacking distances decrease as a function of pressure. Lateral and axial quadruplex compressibilities and force constants have been derived and strong correlation between the strength of tetramer stacking and pressure effects demonstrated. In particular, quadruplex rigidity increases by changing Na^+ to K^+ and by adding excess KCl, as a consequence of increased stacking interactions and quadruplex elongation.

Keywords Quadruplex · Compressibility · High-pressure X-ray diffraction

Introduction

Hierarchical, self-organized structures are frequently observed in biology: initiated at nano scales, they exhibit important properties at macro scale, providing key functions to biological systems (Buehler 2010). In many cases, biological aggregates show an helicoidal organization, which manifests in characteristic physical phenomena. Indeed, helix-specific interactions, elasticity, counter-ion sensitivity, and lyotropic polymorphism have been detected in many biological *molecular* helices, which consist of one or several interwoven helical chains of atoms, but have been also detected in more complex *supramolecular* helices, which are formed upon self-assembly of small molecules. For instance, guanosine quadruplexes, which mimic the structure of chromosome telomeres, microtubules and actin filaments in the cytoskeleton, and some viral particles such as tobacco mosaic virus belong to this class (Kornyshev et al. 2007).

The study of these singular properties in supramolecular helices requires the analysis of the fundamental links between self-structural organizations and properties at multiple scales, from nano to macro (Mariani et al. 2009). Among others, strength and robustness are properties of fundamental importance to biological materials, and are crucial to provide functional properties to living systems and to inspire synthetic and biomimetic materials (Buehler 2010). In particular, strength is defined as the maximum force (or pressure) a material can withstand before breaking, while robustness can be associated to the ability of a material to tolerate flaws and defects in its structural makeup while maintaining its ability to provide functionality (Buehler 2010). In this paper, high-pressure synchrotron X-ray diffraction is used to analyze mechanical properties of quadruplexes obtained by hierarchical self-assembling of alkaline folates, hence to investigate their strength and robustness.

Quadruplex structures have been observed in guanosine-rich single-stranded sequences of DNA [such as in

---

Special Issue: SIBPA 2011 Meeting.

F. Federiconi · E. J. Baldassarri · M. G. Ortore
Università Politecnica delle Marche, Ancona, Italy

M. Mattioni
EBI European Bioinformatics Institute, Cambridge, UK

P. Mariani (✉)
SAIFET Department, Università Politecnica delle Marche,
Via Brecce Bianche, Ancona 60131, Italy
e-mail: mariani@univpm.it

telomeres and other parts of the genome, especially in promoters (Lane et al. 2008; Qin and Hurley 2008)] and in guanosine phosphate and short oligo-guanosine phosphate systems (e.g., guanosine 5′-monophosphate, Gp, deoxyguanosine 5′-monophosphate, d(Gp), and oligo-guanosines such as dGpG and dGpGpG) (Gottarelli et al. 1996). In aqueous solution, the self-assembling of guanosine phosphates is hierarchical (Mariani et al. 2009, 2010). In dilute conditions, the process starts with the formation of tetrameric disks made by four Hoogsteen hydrogen-bonded guanine residues. By increasing the guanosine concentration, and in the presence of nucleating monovalent cations, tetramers stack vertically each on the top of the other at a typical distance of about 3.3 Å (i.e., the same distance existing between stacked base pairs in DNA) and rotated with respect to each other by about 30°. Four-stranded supramolecular helices, named quadruplexes, then result. Despite the absence of covalent bonds along the strand, quadruplexes are rather stable, mainly because cations, which are sandwiched in the inner cavity between two subsequent tetramers, strongly interact with the O_6 ketone groups of eight guanines (four by one tetramer and four by the successive one). By further increasing the concentration, pronounced excluded-volume effects and intermolecular interactions bring about the orientational ordering of the quadruplexes. Indeed, cholesteric (*Ch*) and hexagonal (*H*) columnar phases occur at higher concentrations.

Concerning structural properties, it was observed that the length of the quadruplexes strongly depends on stacking interactions (Mariani et al. 2009, 2010; Franz et al. 1994) and that preferential hydration effects occur during swelling (i.e., the lateral and end-to-end axial inter-helix distances do not change uniformly) (Amaral et al. 1992; Ausili et al. 2004). Moreover, osmotic stress measurements showed that lateral forces dominating at short helix separations (less than few angstroms) are hydrational and that a balance between medium-range attraction, which induces the self-assembly, and short-range repulsion, which prevents the contact between quadruplexes, is implied (Mariani and Saturni 1996; Mariani et al. 1998).

Similarly to guanine, the pterinic heterocyclic ring of the folate molecule, which is a water-soluble B vitamin that occurs naturally in food, shows the same multiple pattern of H-bond donor and acceptor groups. Accordingly, circular dichroism, NMR, and X-ray scattering measurements demonstrated that alkaline folates in water form quadruplexes, following a very similar self-assembling scheme (see Fig. 1) (Ciuchi et al. 1994; Gottarelli et al. 1996). Indeed, folate monomers associate into tetramers (approximately 15.5 Å radius) that stack on top of each other, forming helices with four equally spaced strands (Ciuchi et al. 1994). As observed for guanosine phosphate, quadruplex properties and phase behavior were determined to strongly depend on the alkaline ion involved in the process. For instance, considerable differences were detected for Na_2 folate in pure water and in 1 M NaCl (or KCl) solution (Ciuchi et al. 1994). In pure water, tetramer-tetramer interactions were weak. Indeed, tetramer stacking distances were observed to be strongly influenced by sample composition and temperature: at 30°, the stacking distance increases from about 3.35 to 3.45 Å when the folate weight concentration decreases from 60 to 30%.

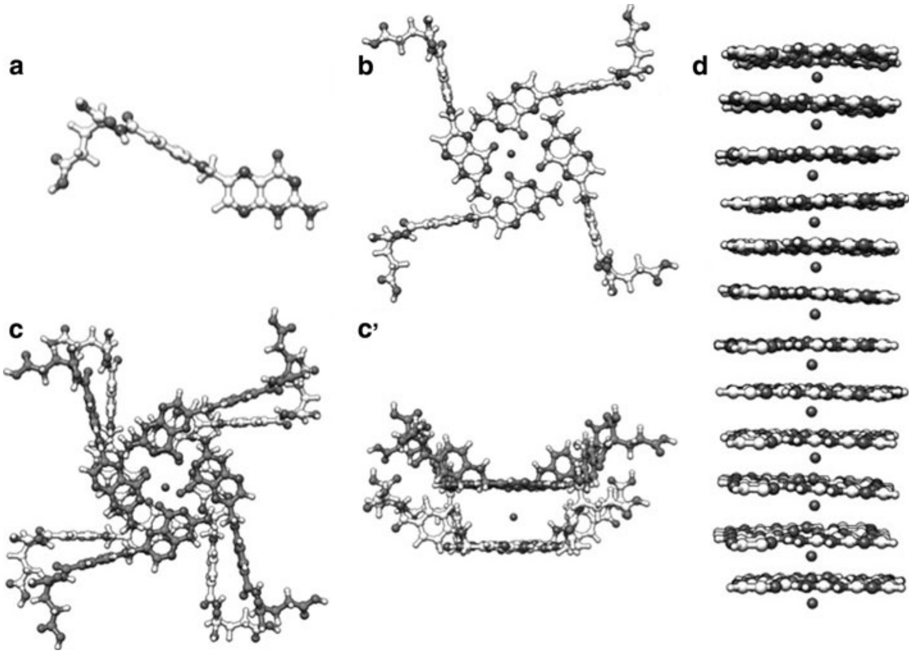

Fig. 1 Self-assembling process: **a** folate molecule; **b** arrangement of the folate tetramer; **c** and **c′** top and lateral views of an octamer, formed by two stacked folate tetramers. The cation is located between the two tetramers; **d** lateral view of a quadruplex, formed by stacking of discrete cation-bound tetramers (folate lateral chains have been omitted for clarity)

Accordingly, the length of the quadruplexes were dependent on the two parameters (in the same concentration range and at the same temperature, the derived quadruplex length decreases from 100 to 15 Å), and only a hexagonal phase was found in the temperature-concentration phase diagram (see Fig. 2, panel a). In 1 M NaCl (or KCl), tetramer-tetramer interactions were stronger, so that, independently of concentration and temperature, a constant tetramer stacking distance of 3.37 Å and the formation of rather stable, 80 Å-long quadruplexes were detected. As a consequence, in addition to the hexagonal phase, a cholesteric columnar phase was observed in the phase diagram (see Fig. 2, panel b) (Ciuchi et al. 1994). Note that the formation of the cholesteric phase (left-handed) is a clear confirmation that the folate quadruplex surface is chiral: the tetramers do not pile up in register, but are continuously rotated one with respect to the other, to generate a supramolecular helix similar to the one observed in homoguanylic oligonucleotides (Proni et al. 2000). However, in the absence of high-resolution structural data, quantitative information on the chirality of the folate quadruplexes cannot be derived.

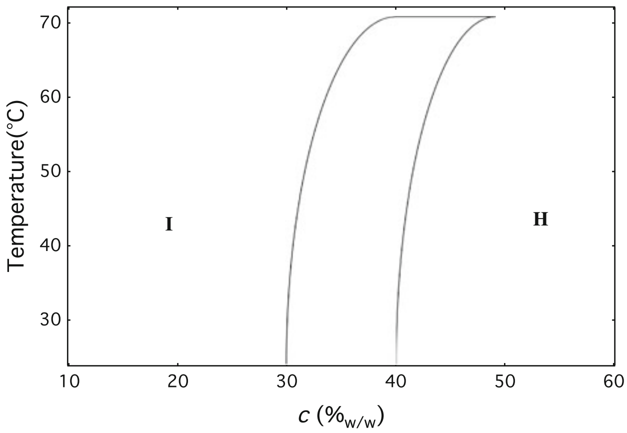

(a) Na$_2$-folate

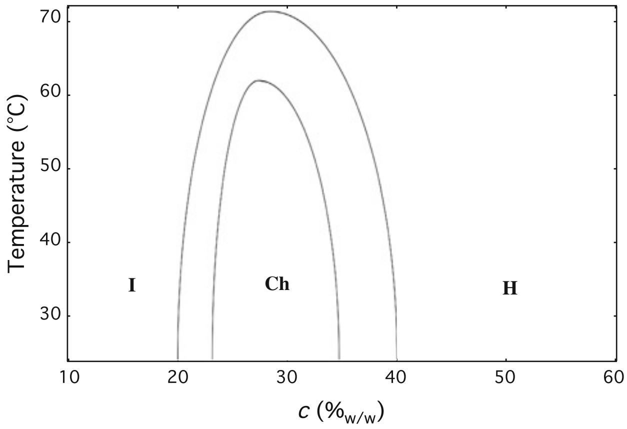

(b) Na$_2$-folate in NaCl 1M

Fig. 2 Na$_2$ folate and Na$_2$ folate in 1 M NaCl phase diagrams (redrawn from Ciuchi et al. 1994)

Structural properties, stability, and energetic of biological systems can be investigated by high-pressure X-ray diffraction (Winter 2002; Spinozzi et al. 2007; Ortore et al. 2009; Rivalain et al. 2010). The recent analysis on quadruplexes formed by guanosine 5′-monophosphate in water showed a lateral inter-helix compressibility that was unusually negative (Ausili et al. 2004), which enforces the original hypothesis that in columnar phases water separates into two regions and suggests that redistribution of water inside the sample occurs during compression. Quadruplex stacking elastic constants were also derived: at fixed ionic strength, a unique elastic constant was detected, while at constant concentration, the fitted elastic constant values confirmed that KCl increases the stacking rigidity. Quadruplex strength appeared then strongly related to stacking stabilization induced by counter-ions.

As stacking interactions are definitely very different and certainly controlled by hydration and counter-ions, the structural, mechanical, and energetic properties of folate quadruplexes have been investigated by high-pressure X-ray diffraction: here, the results obtained by considering Na$^+$ and K$^+$ folate acid salts in the presence and absence of excess K$^+$ ions will be presented.

Materials and methods

Alkaline folates in the form of disodium and dipotassium salts were prepared by neutralization of folic acid (dihydrate, from Sigma) with sodium hydroxide and potassium hydroxide, respectively. Hydrated samples were prepared by mixing the alkaline folates with the required quantities of freshly bidistilled water or aqueous 1 M KCl solution, if requested. Mixtures were left for at least 2 days at 25°C to avoid inhomogeneity. Final folate weight percent concentrations c ranged from 35 to 75%. Note that from nominal composition, the folate volume fraction c_v can be determined using $c_v = c/(c + (100 - c)(v_{wat}/v_{fol}))$, where v_{wat} and v_{fol} are the specific volumes of water and folic acid, respectively. For high-pressure data, volume concentrations were corrected by considering the pressure dependence of densities, as reported in Ausili et al. (2004).

Diffraction experiments were performed at the SAXS beam-line at ELETTRA Synchrotron (Trieste, Italy) at the wavelength $\lambda = 1.54$ Å and in the scattering vector Q-range between 0.035 and 0.70 Å^{-1} $(Q = (4\pi \sin\theta)/\lambda$, where 2θ is the scattering angle). An additional wide-angle X-ray scattering detector was used to measure diffraction patterns in the Q-range from 1.4 to 3.8 Å^{-1}. A pressure cell with diamond windows, which allow the measurement of diffraction patterns at hydrostatic pressures up to 3 kbar, was used (Pressl et al. 1997). Particular attention was applied for checking radiation damage and equilibrium conditions. Measurements were repeated several times at the same constant pressure to account for constant position and intensity of Bragg peaks. Accordingly, samples were gently compressed at a rate of 0.5–2 bar s^{-1} to ensure the onset of equilibrium conditions.

Diffraction patterns were collected at 25°C. Note that no water loss was detected before the hydrated mixtures were mounted into the pressure cell. Moreover, after the X-ray scattering experiments, the water composition of each sample was checked again by gravimetric analysis. The difference between the nominal concentration and the one measured after the pressure cycle was detected to be in the limit of the experimental errors.

Results and discussion

High-pressure X-ray diffraction experiments were performed on K_2 and Na_2 folate samples prepared in water at different hydration conditions and on K_2 folate prepared at different hydrations in 1 M KCl solution. A few X-ray diffraction patterns are reported in Fig. 3.

As a first result, it can be observed that pressure induces small, but continuous variations in the position of the Bragg peaks (which move towards higher Q-values). In nearly every case, the spacing ratios of the narrow peaks detected in the low-angle diffraction region index to a two-dimensional hexagonal lattice and indicate that the structure is hexagonal. From the peak position, $Q_{h,k}$, the unit cell dimension, a (i.e., the inter-axial distance between the quadruplexes), can be obtained by using (Luzzati 1968):

$$a = (4\pi/\sqrt{3})\,\frac{\sqrt{h^2 + k^2 - hk}}{Q_{h,k}} \tag{1}$$

Instead, X-ray diffraction profiles obtained from low-concentration samples of K_2 folate in 1 M KCl are characterized by a low-angle broad band, which confirms the presence of a cholesteric phase (see Fig. 2). Moreover, the cholesteric phase has been detected also in low-concentration K_2 folate samples, but in equilibrium with the hexagonal phase. In such cases, the hexagonal phase disappears as a function of pressure.

Wide-angle diffraction profiles give experimental evidence on the columnar nature of the phase. Indeed, a narrow band is observed in all investigated samples in the wide-angle diffraction region at about $Q = (2\pi/3.3)\ \text{Å}^{-1}$; according to previous works (Franz et al. 1994; Amaral et al. 1992), this reflection is related to the vertical stacking of tetramers inside the quadruplexes. From the peak position, the distance between the stacked tetramers, b, can be obtained. No extra low-angle peaks were observed in the

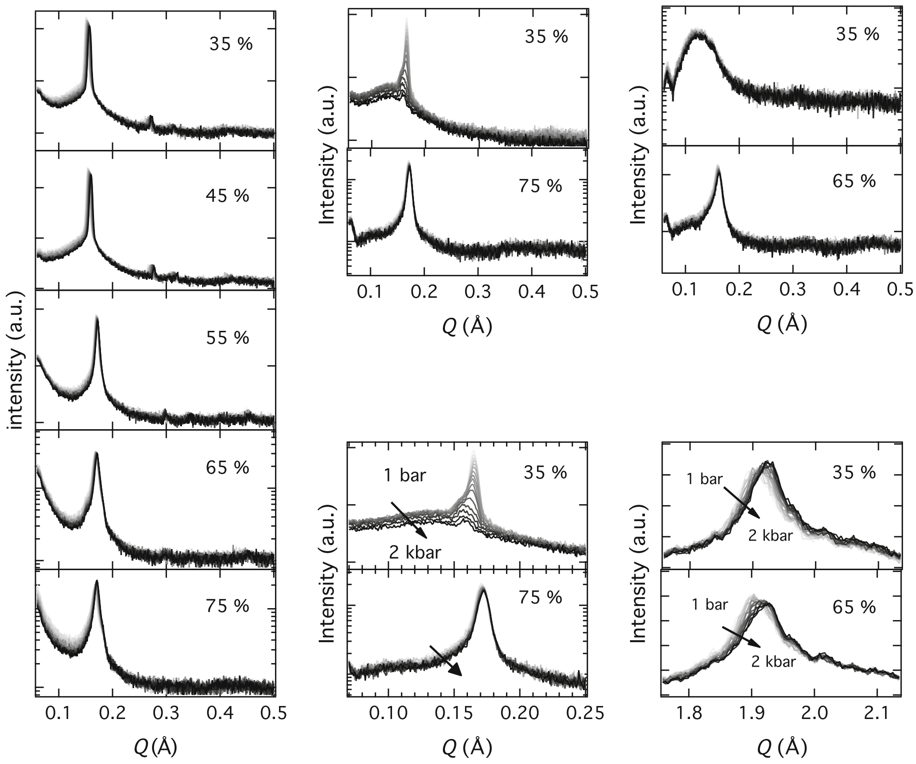

(a) Na_2-folate **(b)** K_2-folate **(c)** K_2-folate in KCl

Fig. 3 X-ray diffraction results obtained at different concentrations (as reported in the frames) and as a function of pressure (from 1 to 2,000 bar). *Left column*: low-angle profiles referring to Na_2 folate. *Central column*: X-ray diffraction profiles referring to K_2 folate. *Top frames*, low-angle profiles observed at two different concentrations; low frames, enlargement of the low-angle region, to accentuate the pressure effect. *Right column*: X-ray diffraction profiles referring to K_2 folate prepared in 1 M KCl solution. *Top frames*, low-angle profiles observed at two different concentrations; *low frames*, enlargement of the corresponding high-angle regions, to evidence the pressure effect diffraction patterns, indicating the absence of smectic-like order. As expected, in fact, no long-range column-column correlation of the tetramer position exists, as the rods may freely translate in a direction perpendicular to the two-dimensional hexagonal cell.

Some quantitative results are reported in Fig. 4, where the inter-helical distance between the quadruplexes and the tetramer stacking distance are reported as a function of pressure. As general results, at all concentrations and for all considered samples (Na_2 folate, K_2 folate and K_2 folate in 1 M KCl), inter-helical and stacking distances decrease rather linearly under compression. Pressure dependence appears to be related to sample concentration and composition. In particular, because of the presence of the cholesteric phase, unit cells extend in a larger range in K_2 folate prepared both in pure water and in 1 M KCl. In addition, while in pure water the distance between stacked tetramers increases as a function of water content, in excess KCl the stacking distance does not change with hydration, confirming that excess counter-ions induce stronger tetramer interactions (Ciuchi et al. 1994).

Lateral and axial compressibilities. A linear fit to the unit cell parameters has been used to calculate the pressure dependence of stacking and inter-helical distances and the corresponding 1D, axial, and 2D, lateral compressibilities, β_{1D} and β_{2D}, respectively:

$$\beta_{1D} = -1/b(db/dP) \text{ and } \beta_{2D} = -1/\sigma(d\sigma/dP) \qquad (2)$$

being $\sigma = a^2\sqrt{3}/2$.

Compressibility data obtained for the different samples are reported in Fig. 5: in all cases both lateral and axial compressibilities are positive, and increase with increasing water concentration. Furthermore, while compressibilities for the two folate salts are almost identical, the presence of excess KCl appears to strongly reduce both pressure and concentration dependence. It should be noticed that direct lipid hexagonal phases, such as in dodecyl-tri-methyl-ammonium cloride and lyso-oleoyl-phosphatidyl choline systems, show very similar β_{2D} value and pressure dependence (Paccamiccio et al. 2006, Pisani et al. 2003), but remarkable differences exist from the compressibilities previously obtained from quadruplexes formed by guanosine 5′-monophosphate (Ausili et al. 2004). Indeed, guanosine hexagonal phases show *negative* β_{2D} values (e.g., inter-helical distances increase as a function of pressure).

Fig. 4 Pressure dependence of the lateral inter-helix (**a**) and tetramer stacking (**b**) distances for the different investigated samples. Concentrations are indicated in the *graph*; in the case of partial overlapping, the *arrow* shows the increasing concentration. *Lines* are linear fit to the data

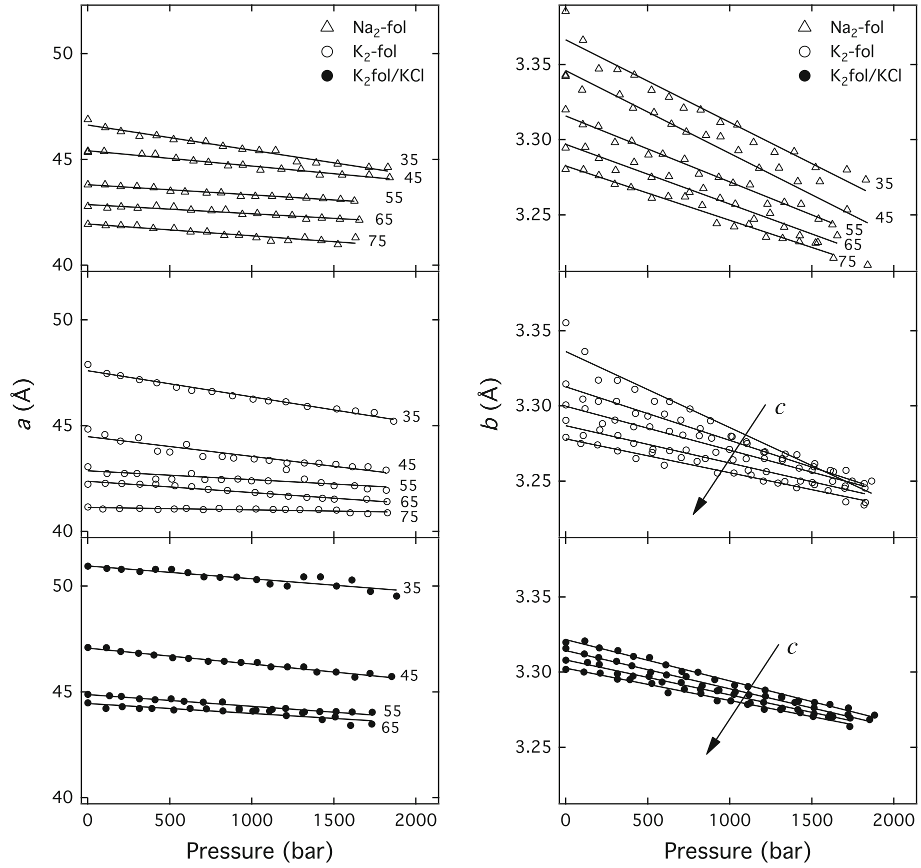

(a) hexagonal unit cell **(b)** stacking distance

Fig. 5 Pressure dependence of 2D lateral (β_{2D}) and 1D axial (β_{1D}) compressibilities as obtained for the different investigated samples. Concentrations and *symbols* as in Fig. 4. *Lines* are guides for the eye

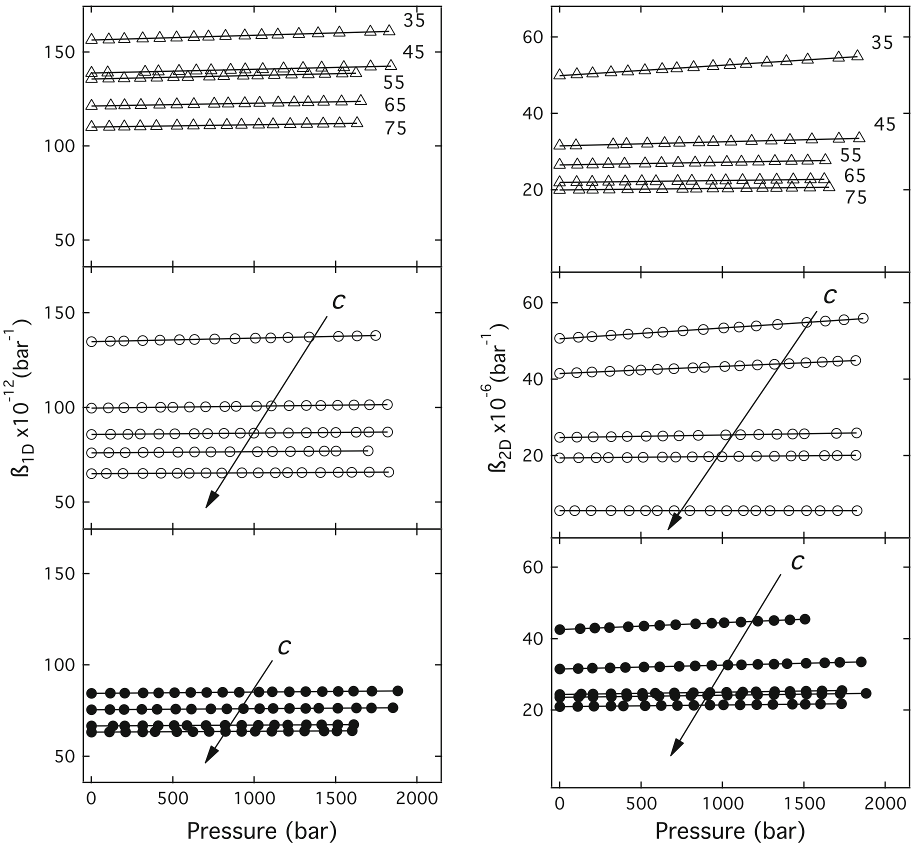

(a) lateral compressibility **(b)** axial compressibility

Three-dimensional unit cell decomposition. High-pressure X-ray diffraction experiments on quadruplexes formed by alkaline folates show that both inter-helical lateral and tetramer stacking distances decrease as a function of pressure. From these data, axial and lateral compressibilities have been calculated, as shown in Fig. 5. Both are positive, but lateral compressibilities converge to very low values for increasing concentration.

Before entering into the force analysis, one point should be discussed. In fact, previous results demonstrated that the quadruplex length depends on counter-ions and on the presence of excess salt (Mariani et al. 2009, 2010; Ausili et al. 2004). Indeed, because of the formation of finite but longer quadruplexes, a cholesteric phase is observed in K_2 folate as well as in K_2 folate in 1 M KCl. It is obvious that this fact should reflect on compressibility values. According to the packing model reported in Fig. 6, *L*/*C* values ($L/C = a^2(\sqrt{3}/2)c_v/(\pi R^2)$) have been calculated as a function of pressure. Because the complement of the *L*/*C* ratio essentially gives the fraction of water in the axial direction (the unity ratio indicates infinitely long rods), the comparison of data reported in Fig. 7 confirms that only small differences occur between K_2 and Na_2 folates, whereas longer quadruplexes form in the presence of excess salt. Moreover, *L*/*C* data show that the fraction of water in the axial direction slightly increases during compression, suggesting that a change in the local sample composition occurs, with a redistribution of water from the lateral to the axial region.

Further information can be derived considering a series of volume-per-tetramer parameters. Indeed, the average length of a quadruplex can be written as $L = nb$, where n is the average number of stacked tetramers (see Fig. 6). Accordingly, the 3D unit cell volume-per-tetramer, $V/n = a^2(\sqrt{3}/2)C/n$, can be decomposed and written as the sum of terms corresponding to the volume of one tetramer, $V_{fol,4}$, to the volume of water located in the lateral region around each tetramer, $V_{w,lat}$, and to the volume of water situated in the axial region, normalized to n tetramers, $V_{w,ax}$:

$$V/n = V_{fol,4} + V_{w,lat} + V_{w,ax} = \pi R^2 b/c_v$$

$$V_{fol,4} = \pi R^2 b \tag{3}$$

$$V_{w,lat} = a^2 b(\sqrt{3}/2) - \pi R^2 b \tag{4}$$

$$V_{w,ax} = V/n - a^2 b(\sqrt{3}/2) \tag{5}$$

Since *V*/*n* can be easily derived, unit cell decomposition leads to results reported in Fig. 8 as a function of pressure. It can be observed that while the *V*/*n* values are quite

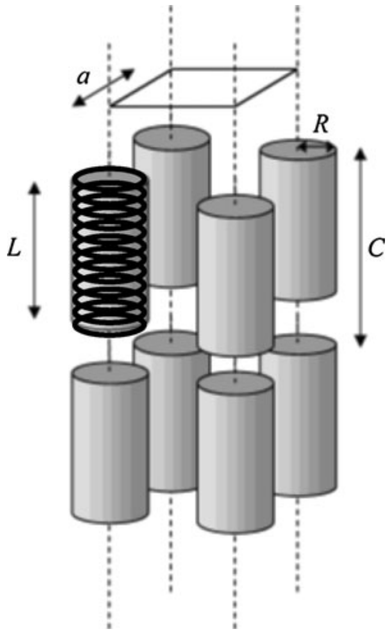

Fig. 6 Model for the hexagonal packing of finite quadruplexes: the rod-like particles of constant cross-sectional radius R = 15.5 Å (Ciuchi et al. 1994) and average length L are packed in a 3D hexagonal cell. a is the lateral inter-helical distance and C is the average distance between the rod centers in the axial direction, normal to the 2D hexagonal cell plane

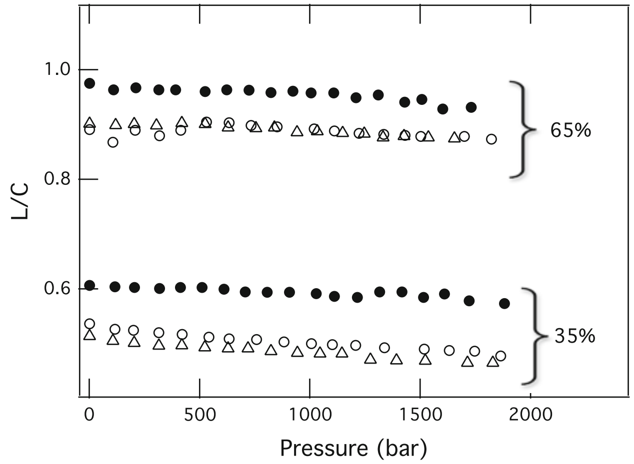

Fig. 7 Pressure dependence of the *L/C* ratio, calculated at two different concentrations for the different investigated samples. *Symbols* as in Fig. 4; *c* values are indicated in the *graph*

similar, strong differences occur in the water distribution inside the cell. The comparison proves that excess salt induces a strong increase of the volume of water in the lateral region, at the expense of the corresponding volume in the axial region. Similar effects differentiate K_2 folate to Na_2 folate results, even if variations are very small and more evident in the more hydrated samples. The changes occurring during compression in the local sample composition via redistribution of water from the lateral to the axial region are then confirmed: indeed, the volume of water per tetramer in the lateral region shows a negative dependence on pressure, while $V_{w,ax}$ increases during compression.

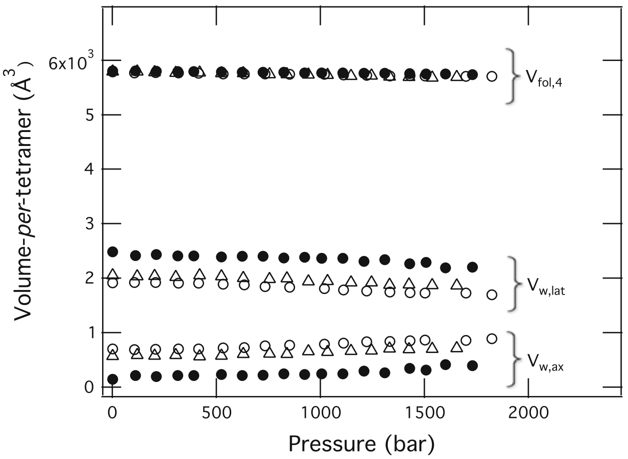

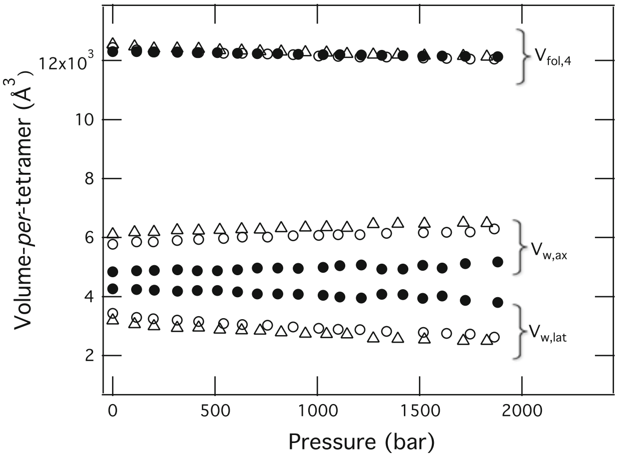

Fig. 8 Pressure dependence of volume-*per*-tetramer parameters (tetramer volume, $V_{fol,4}$, volume of water in the lateral region around each tetramer, $V_{w,lat}$, and volume of water in the axial region, $V_{w,ax}$), derived at two different concentrations (c = 35%, *lower graph*; c = 65%, *upper graph*) for the different investigated samples. *Symbols* as in Fig. 4

It should be noticed that water redistribution *from the axial to the lateral interhelical region* was suggested to occur in the guanosine 5′-monophosphate system during compression. According to the present results, it appears evident that the relative amount of water in the axial and lateral regions (see Fig. 6) is controlled by the balance between repulsive and attractive inter-helix lateral forces, a balance dependent on pressure in different ways. It has been reported that pressure induces volume reduction in DNA by determining better base stacking (in particular, of the bases located at the ends of the helices, which are expected to be less stable) (Balny et al. 2002). As the behavior is opposite to the situation observed in most biological systems [where increased hydrostatic pressure leads to dissociation (Silva et al. 1996), mainly because bound water has a slightly higher density than bulk water and then a system under compression tries to create more surface], it has been argued that water close to the DNA bases should have slightly lower density (Balny et al. 2002) or that the more suitable stacking is associated with an increased electrostriction of water due to counter-ion release (Prehoda and Markley 1996). Closer (and better) base stacking is clearly induced by pressure in the folate samples here investigated (see Fig. 4), but it was also detected in the guanosine 5′-monophosphate system (Ausili et al. 2004): the correlated negative volume changes can have different origins, but it is evident that according to the hydration force scheme (Mariani et al. 1998; Kornyshev and Leikin 1998) any change in distribution of charges and bound counter-ions on the helix surface will affect the balance between repulsive and attractive lateral forces (Kornyshev et al. 2007). A net inter-helix attraction (repulsion) could result because of favorable (unfavorable) surface charge distribution patterns determined by closer tetramer stacking. In the folate system, attraction is induced by pressure, and the distance between quadruplexes decreases on compression; accordingly, water redistribution from the lateral to the axial region occurs. In the guanosine 5′-monophosphate system, where stacking forces are stronger, repulsion is increased by pressure, so that under compression the lateral distance increases, and water redistribution in the opposite direction takes place (Ausili et al. 2004).

Force constant analysis. According to unit cell decomposition, the force-per-unit length between nearest quadruplex pairs, the interaction of which is taken to be pairwise additive, *f*(*a*), can be derived by using (Rau et al. 1984):

$$f(a) = Pa/\sqrt{3} \tag{6}$$

The forces between quadruplexes, as derived from data reported in Fig. 4, are shown in Fig. 9. At large interaxial distances (⩾35–40 Å for DNA molecules), force magnitudes and slopes are expected to mainly arise from fluctuation-enhanced electrostatic repulsion (Israelachvili 1994). In the case of parallel cylindrical particles, as linear polyelectrolyte molecules in solution, the force can be approximated by (Rau et al. 1984; Israelachvili 1994):

$$F_{el}(a) = F_0 \frac{e^{-a/\lambda_D}}{\sqrt{a/\lambda_D}} \tag{7}$$

where the force coefficient F_0 is independent of the axis-to-axis distance a, and λ_D is the Debye length.

Due to the strong dependence on torsional fluctuations and inherent torsional flexibility of the unlinked stacks of tetramers, no helix-specific interactions are expected beyond 5–10 Å surface separation in folate quadruplexes (Kornyshev et al. 2007), and none have been in fact observed in guanosine-phosphate quadruplexes (Mariani and Saturni 1996). Therefore, forces derived by Eq. 6 should agree with the Poisson-Boltzmann theory for homogeneously charged cylinders over the whole range of distances examined, and Eq. 7 can be used to derive lateral force parameters.

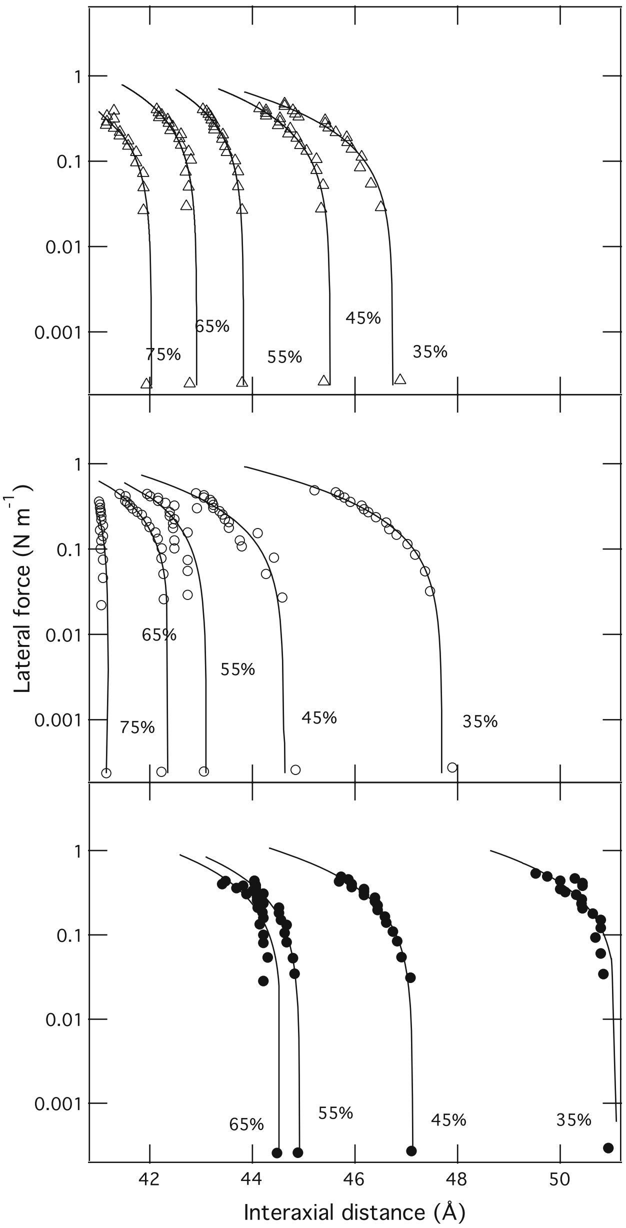

Fig. 9 Pressure dependence of force-per-unit length between nearest quadruplexes. *Top frame*, Na_2 folate; *central frame*, K_2 folate; lower frame, K_2 folate in 1 M KCl solution. *Lines* are best-fit curves obtained using Eq. 7. Concentrations are indicated in the *graphs*

Fitting curves by Eq. 7 are superposed to experimental points in Fig. 9. Since fitting parameters resulted practically independently of concentration, average values are reported in Table 1. It can be observed that final results on the different samples are very similar and that an excess salt does not produce a relevant reduction of the magnitude of the Debye length. Considering the observed increase in *L*/*C* and the changes in the volume-per-tetramer parameters, it can be suggested that extra potassium is mainly involved in the elongation of quadruplexes and does not modify the properties of the aqueous medium. On the other hand, the small changes in the force coefficient F_0 could indicates that helix surface properties (as charge or potential) are changing.

The cell decomposition approach also applies in the derivation of the quadruplex axial elastic constant. Indeed, the energetic cost per tetramer associated with the isothermal compression can be calculated by numerical integration of the external pressure P over the volume of one tetramer $V_{fol,4}$. By definition,

$$\Delta G^* = -\mathcal{N}_A \int P dV_{fol,4} \tag{8}$$

where $\mathcal{N}_A$ is Avogadro's number and ΔG^* is the change in free energy per mole of folate tetramers during helix compression. ΔG^* values for the different investigated samples are shown in Fig. 10, as a function of stacking distance (which in turn depends on pressure). Noticeable is the considerable dependence on sample composition (water content and kind and amount of counter-ion) of the ΔG^* changes (indeed, free-energy changes include the work for transferring water molecules from the lateral to the axial inter-helix regions, and thus should depend on the *L*/*C* parameter). Moreover, the ΔG^* magnitude appears very close to the strength of the van der Waals interactions (about 10^3 J mol^{-1}; note that hydrogen bonds lie between 10×10^3 and 40×10^3 J mol^{-1}).

In a first approximation, the observed changes in free energy can be expected to originate mainly from interactions between adjacent base tetramers; the first term in the ΔG^* expansion should be related to the stacking distance. As previously considered (Ausili et al. 2004), the classical form of the elastic energy of a spring can be then used to describe the macroscopic cost to compress the quadruplex:

$$\Delta G_e^* = \frac{\mathcal{N}_A}{2} k (b - b_0)^2 \tag{9}$$

where k is the elastic constant. Best-fit curves obtained using Eq. 9 are superposed to experimental data in Fig. 10, while fitting parameters are reported in Fig. 11. Describing the compression work only in terms of stacking elasticity is certainly a crude simplification, but a few comments can be reported. Concerning b_0, the large increase of the equilibrium stacking repeat distance on hydration suggests that interactions between piled tetramers are unusually weak (and Na < K). However, the more constant b_0 values observed in KCl solution indicate that excess salt induces

Table 1 Lateral force fitting results

System	F_0 (nN/nm)	λ_D(Å)
Na_2-fol	(7.4 ± 0.5) × 10^3	6.1 ± 0.6
K_2-fol	(8.8 ± 0.6) × 10^3	5.9 ± 0.8
K_2-fol/KCl	(6.1 ± 0.5) × 10^3	6.7 ± 0.5

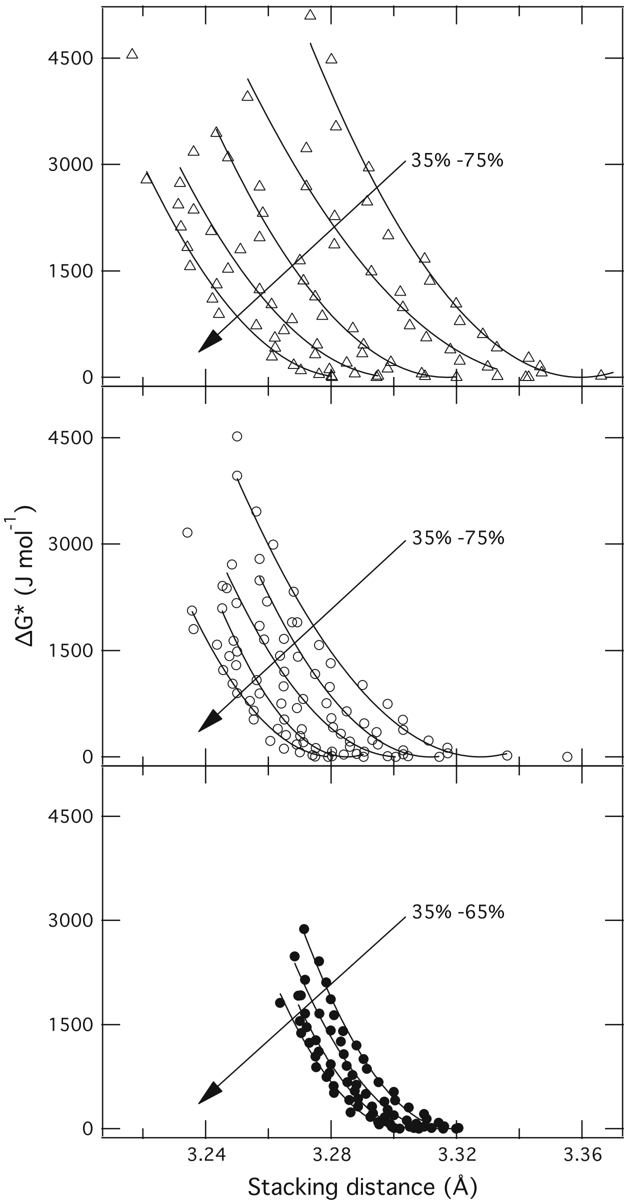

Fig. 10 Changes in the free energy per tetramer, ΔG^*, during quadruplex compression. *Top frame*, Na_2 folate; *central frame*, K_2 folate; *lower frame*, K_2 folate in 1 M KCl solution. *Lines* are best-fit curves obtained using Eq. 9. Concentrations are indicated by the *arrows*

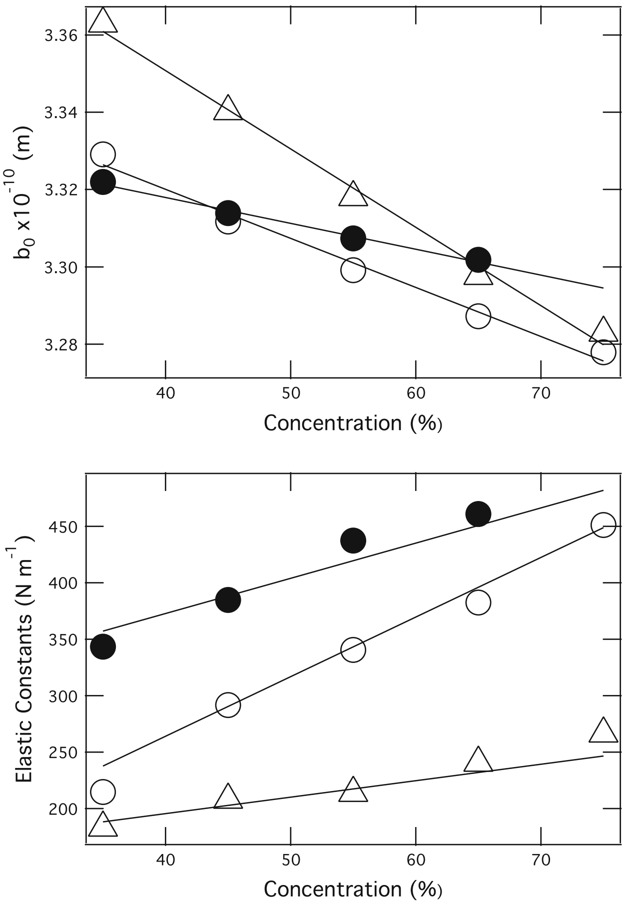

Fig. 11 Elastic energy fitting parameters. *Symbols* as in Fig. 4. *Lines* are guides for the eye

stronger tetramer interactions. Taking into account the *L*/*C* behavior, it can be concluded that stronger tetramer interactions are reflected in stronger aggregation, and then in the formation of longer quadruplexes.

The strength of tetramer stacking interactions is also reflected in the elastic constants. Indeed, the fitted *k* values are significantly lower than those observed in the guanosine 5′-monophosphate/water system [385 nN nm^{-1}, in Gp in pure water, *c* from 70 to 90% and 469 nN nm^{-1} Gp in 2 M KCl, $c = 70\%$ (Ausili et al. 2004)], in which stacking interactions are undoubtedly strong (Mariani et al. 2009). Because of the weak stacking interactions, *k* values are very sensitive to sample composition. On one side, hydration makes stacking interactions weaker, softening the quadruplexes. On the other, the used counter-ions, which are known to be essential for the stability of the supramolecular aggregates by enhancing base-stacking interactions, modify the dependency. As already suggested by phase diagrams (Fig. 2), Na$^+$ ions do not provide a sufficient strong aggregation, so that quadruplexes are relatively short and rather soft. The situation slightly changes for K_2 folate: the stronger tetramer interactions determined by K$^+$ ions increase the quadruplex length (see *L*/*C* ratios) and rigidity, which is reflected in the observed hardening. Accordingly, the addition of excess salt in solution induces the appearance of a cholesteric phase (see Fig. 2). On the basis of the approach developed by Taylor and Herzfeld (1993), a stable nematic phase intervening between the isotropic and the hexagonal phases can be found when finite rigid aggregates are on average sufficiently elongated. The obtained elastic constants (which show values very similar to those observed in Gp) confirm that excess KCl determines sufficiently strong aggregation and the rigidity required for the appearance of cholesteric phase.

Conclusions

Quadruplexes made by alkaline folates have been investigated by high-pressure X-ray diffraction. In folate quadruplexes, tetramer-tetramer interactions are definitively weak, so that subtle effects due to different alkaline ions can be easily monitored. Structural data show that both inter-helical lateral and tetramer stacking distances decrease as a function of pressure. Results have been analyzed in terms of lateral and axial quadruplex compressibilities and force constants, evidencing a strong correlation between the strength of tetramer stacking and pressure effects. In particular, the analysis of the measured free energy changes during compression demonstrated that quadruplex rigidity increases by changing Na$^+$ to K$^+$ and by adding excess KCl, as a consequence of increased stacking interactions and quadruplex elongation. Stronger tetramer interactions may be attributed to a specific interaction of K$^+$ ions, which probably have the right size to keep together the stacked tetrameric planes. Subsequent effects are the observed constancy of tetramer stacking distance and of the aggregate length with concentration and pressure and the increased rigidity.

In conclusion, this work shows that an appropriate understanding of relationships between self-structural organizations and properties at multiple scales can be obtained by analyzing few mechanical and thermodynamic parameters when pressure and concentration vary. Such an approach can then provide information to living systems and to inspire synthetic and biomimetic materials, as could happen in setting the best strategy to stabilize natural quadruplex structures at 3′ single-stranded telomeric overhangs and then to block telomerase from lengthening the telomere, which has been demonstrated to be a promising approach to cancer therapy (Tahara et al. 2006), or in the synthesis of long and stable nanowires formed for instance by guanine (Changenet-Barret et al. 2010) or folate tetrads.

Acknowledgments We gratefully acknowledge funding from the Italian Ministry of Education, University and Research (MIUR) through the PRIN project "Self-assembling and structural properties of guanosine derivatives in aqueous solutions" (code 2008F3734A). We thank Milos Steinhart and Heinz Amenitsch for experimental assistance.

References

Amaral LQ, Itri R, Mariani P, Micheletto R (1992) Structural study of the aggregates formed by the dinucleoside phosphate G2 in aqueous solution. Liq Cryst 12:913–919

Ausili P, Pisani M, Finet S, Amenitsch H, Ferrero C, Mariani P (2004) Pressure effects on columnar lyotropics: anisotropic compressibilities in guanosine monophosphate four-stranded helices. J Phys Chem 108:1783–1789

Balny C, Masson P, Heremans K (2002) High pressure effects on biological macromolecules: from structural changes to alteration of cellular processes. Biochim Biophys Acta 1595:3–10

Buehler MJ (2010) Computational and theoretical materiomics: properties of biological and de novo bioinspired materials. J Comput Theor Nanosci 7:1203–1209

Changenet-Barret P, Emanuele E, Gustavsson T, Improta R, Kotlyar AB, Markovitsi D, Vay IO, Zakrzewska K, Zikich D (2010) Optical properties of guanine nanowires: experimental and theoretical study. J Phys Chem C 114:14339–14346

Ciuchi F, Di Nicola G, Franz H, Gottarelli G, Mariani P, Ponzi Bassi MG, Spada GP (1994) Self-recognition and self-assembly of folic acid salts: Columnar liquid crystalline polymorphism and the column growth process. J Am Chem Soc 116:7064–7071

Franz H, Ciuchi F, Di Nicola G, De Morais MM, Mariani P (1994) Unusual lyotropic polymorphism of deoxyguanosine-5-monophosphate: X-ray diffraction analysis of the correlation between self-assembling and phase behavior. Phys Rev E 50:395–402

Gottarelli G, Mezzina E, Spada GP, Carsughi F, Nicola GD, Mariani P, Sabatucci A, Bonazzi S (1996) The self-recognition and self-assembly of folic acid salts in isotropic water solution. Helvetica Chimica Acta 79:220–234

Gottarelli G, Spada G, Mariani P (1996) The self-assembly of guanosine derivatives and folic acid. In: Crystallography of supramolecular compounds. Kluwer, Dordrecht

Israelachvili JN (1994) Intermolecular and surface forces. Academic Press, London

Kornyshev AA, Leikin S (1998) Erratum: theory of interaction between helical molecules. [J. Chem. Phys. 107, 3656 (1997)]. J Chem Phys 108:7035

Kornyshev AA, Lee DJ, Leikin S, Wynveen A (2007) Structure and interactions of biological helices. Rev Mod Phys 79:943–996

Lane AN, Chaires JB, Gray RD, Trent JO (2008) Stability and kinetics of G-quadruplex structures. Nucleic Acids Res 36:5482–5515

Luzzati V (1968) X-ray diffraction studies of lipid-water systems. In: Chapman D (ed) Biological membranes. Academic Press, London

Mariani P, Saturni L (1996) Measurement of inter-columnar forces between parallel guanosine four stranded helices. Biophysical J 70:2867–2874

Mariani P, Ciuchi F, Saturni L (1998) Helix-specific interactions induce condensation of guanosine four stranded helices in concentrated salt solutions. Biophysical J 74:430–435

Mariani P, Spinozzi F, Federiconi F, Amenitsch H, Spindler L, Drevensek-Olenik I (2009) Small angle X-ray scattering analysis of deoxyguanosine 5′-monophosphate self-assembing in solution: nucleation and growth of G-quadruplexes. J Phys Chem B 113:7934–7944

Mariani P, Spinozzi F, Federiconi F, Ortore MG, Amenitsch H, Spindler L, Drevensek-Olenik I (2010) Guanosine quadruplexes in solution: a small-angle X-ray scattering analysis of temperature effects on self-assembling of deoxyguanosine monophosphate. J Nucleic Acids. Article ID 472478

Ortore MG, Spinozzi F, Mariani P, Paciaroni A, Barbosa LRS, Amenitsch H, Steinhart M, Ollivier J, Russo D (2009) Combining structure and dynamics: non-denaturing high-pressure effect on lysozyme in solution. J R Soc Interface 6:S619–S634

Paccamiccio L, Pisani M, Spinozzi F, Ferrero C, Finet S, Mariani P (2006) Pressure effects on lipidic direct phases: the dodecyltrimethyl ammonium chloride-water system. J Phys Chem B 110:12410–12418

Pisani M, Narayanan T, Gregorio GMD, Ferrero C, Finet S, Mariani P (2003) Compressing inverse lyotropic systems: Structural behavior and energetics of dioleoyl phosphatidyl ethanolamine. Phys Rev E 68:021924

Prehoda KE, Markley JL (1996) Use of partial molar volumes of model compounds in the interpretation of high pressure effects on proteins. In: Markley JL, Northrop DB, Royer CA (eds) High-pressure effects in molecular biophysics and enzymology. Oxford University Press, Oxford

Pressl K, Kriechbaum M, Steinhart M, Laggner P (1997) High pressure cell for small- and wide-angle X-ray scattering. Rev Sci Instrum 68:4588–4592

Proni G, Gottarelli G, Mariani P, Spada GP (2000) The chirality of the cholesteric phase of DNA and G-wires: its connection to their molecular structures. Chem Euro J 6:3249–3253

Qin Y, Hurley LHH (2008) Structures, folding patterns, and functions of intramolecular DNA G-quadruplexes found in eukaryotic promoter regions. Biochimie 90:1149–1171

Rau DC, Lee B, Parsegian VA (1984) Measurement of the repulsive force between polyelectrolyte molecules in ionic solution: hydration forces between parallel DNA double helices. Proc Natl Acad Sci USA 81:2621–2625

Rivalain N, Roquain J, Demazeau G (2010) Development of high hydrostatic pressure in biosciences: Pressure effect on biological structures and potential applications in biotechnologies. Biotechnol Adv 28:659–672

Silva J, Foguel D, Poian ATD, Prevelige PE (1996) The use of hydrostatic pressure as a tool to study viruses and other macromolecular assemblages. Curr Opin Struct Biol 6:166–175

Spinozzi F, Mariani P, Saturni L, Carsughi F, Bernstorff S, Cinelli S, Onori G (2007) Met-myoglobin association in dilute solution during pressure-induced denaturation: an analysis at pH 4.5 by high-pressure small-angle X-ray scattering. J Phys Chem B 111:3822–3830

Tahara H, Shin-ya K, Seimiya H, Yamada H, Tsuruo T, Ide T (2006) G-quadruplex stabilization by telomestatin induces TRF2 protein dissociation from telomeres and anaphase bridge formation accompanied by loss of the 3′ telomeric overhang in cancer cells. Oncogene 25:1955–1966

Taylor M, Herzfeld J (1993) Liquid-crystal phasesof self-assembled molecular aggregates. J Phys Condens Matter 5:2651–2678

Winter R (2002) Synchrotron X-ray and neutron small-angle scattering of lyotropic lipid mesophases, model biomembranes and proteins in solution at high pressure. Biochim Biophys Acta Protein Struct Mol Enzymol 1595:160–184